Supporting Information:

Nonuniform Composition Profiles in Amorphous Multimetal Oxide Thin Films Deposited from Aqueous Solution

Keenan N. Woods,[†] Milana C. Thomas,[‡] Gavin Mitchson,[†] Jeffrey Ditto,[†] Can Xu,[§] Donna Kayal,[†] Kathleen C. Frisella,[†] Torgny Gustafsson,[§] Eric Garfunkel,[∥] Yves J. Chabal,[‡] David C. Johnson,[†] Catherine J. Page[*,†]

[†]Department of Chemistry & Biochemistry and Materials Science Institute, University of Oregon, Eugene, Oregon 97403, United States

[‡]Department of Materials Science and Engineering, University of Texas at Dallas, Richardson, Texas 75080, United States

[§]Department of Physics and Astronomy and [∥]Department of Chemistry and Chemical Biology, Rutgers University, Piscataway, New Jersey 08854, United States

*cpage@uoregon.edu

Figure S1: Fourier transform infrared (FTIR) spectra

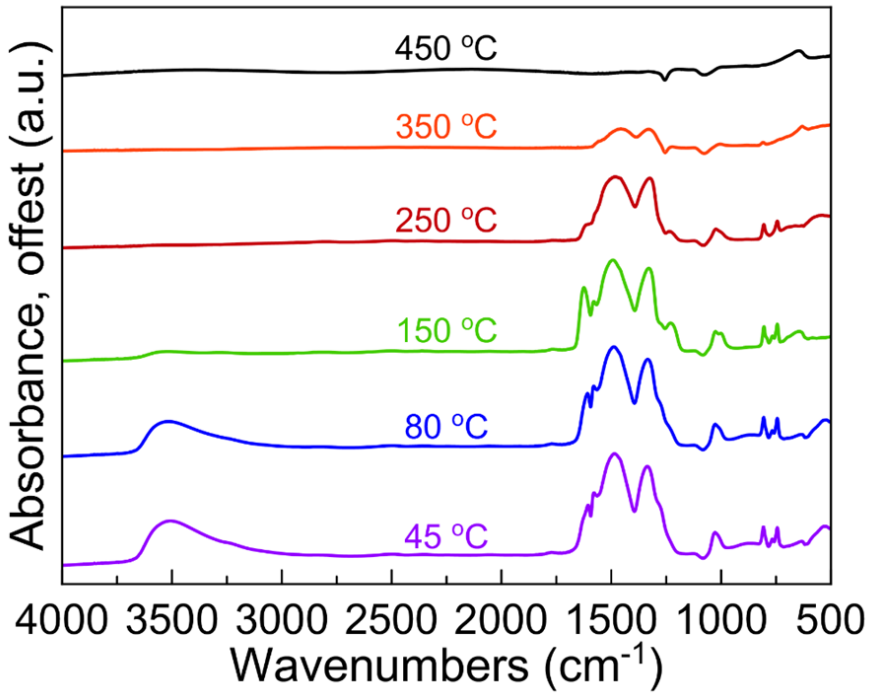

Figure S1. FTIR spectra of a single-layer LZO film deposited from a 1.00 M precursor solution sequentially heated in situ to various annealing temperatures.

X-ray reflectivity (XRR) modeling procedure

The XRR spectra were fit using Bede REFS software, which generates a solution based on an initial model input and a genetic algorithm to minimize residuals. Two types of model inputs were used: a homogeneous, single-layer model and a model with multiple layers informed by HAADF-STEM studies. An approximate total thickness of 40 nm was used as an initial starting thickness for each model. For the more complex models, the thickness of the individual layers was approximated from the HAADF-STEM images in Figure 2. In all cases, the thickness, density, and roughness of each individual layers were allowed to vary independently. After producing the best fit, the models were perturbed to ensure that they had each settled in a global minimum. Goodness of Fit (GOF) values were output by the modeling program and indicate the quality of the model fitting.

Figure S2: XRR homogeneous single-layer best fit models

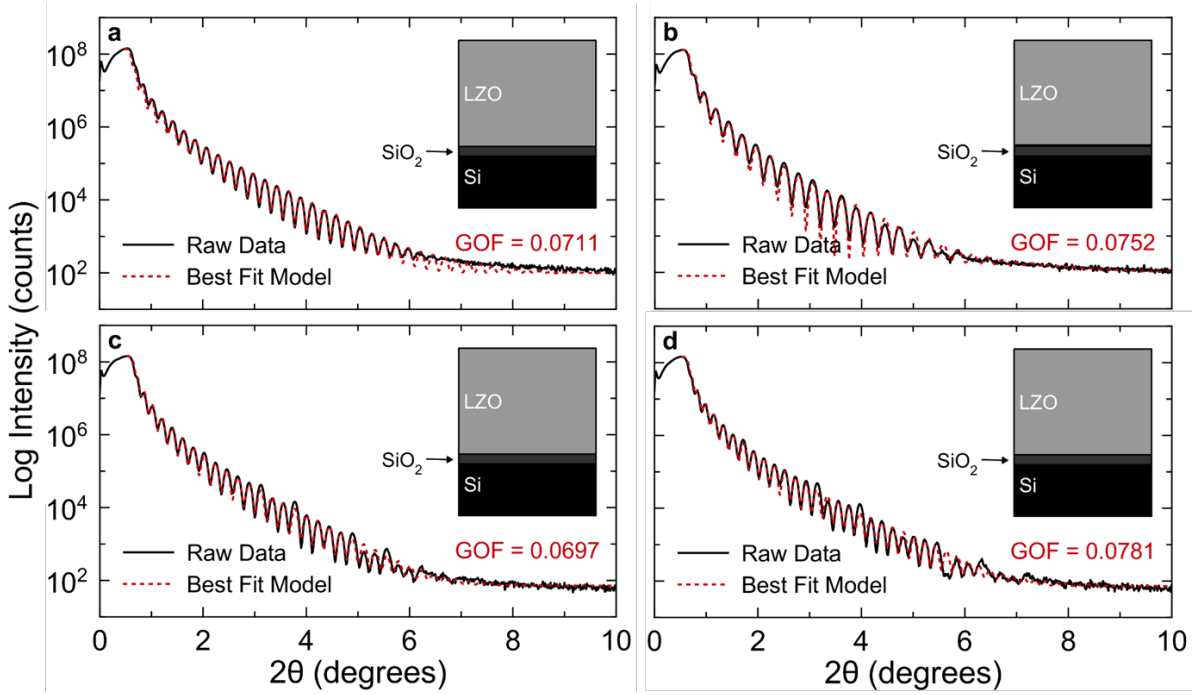

Figure S2. Single-layer models fit to XRR data collected from (a) one-, (b) two-, (c) three-, and (d) four-coat films deposited from 1.00, 0.50, 0.33, and 0.25 M precursor solutions, respectively.

Table S1: XRR single-layer best fit model parameters

	Single-Layer Best Fit Parameters		
Layer(s)	***t* (nm)**	***D* (g cm^{-3})**	***R* (nm)**
1L Film			
LZO	38.0	5.83	0.3
2L Film			
LZO	31.1	6.04	0.5
3L Film			
LZO	39.2	5.89	0.4
4L Film			
LZO	41.7	5.95	0.4

Table S1. XRR single-layer best fit model parameters [thickness (*t*), density (*D*), roughness(*R*)] for XRR data and models presented in Figure S2.

Figure S3: XRR inhomogeneous multilayer best fit models

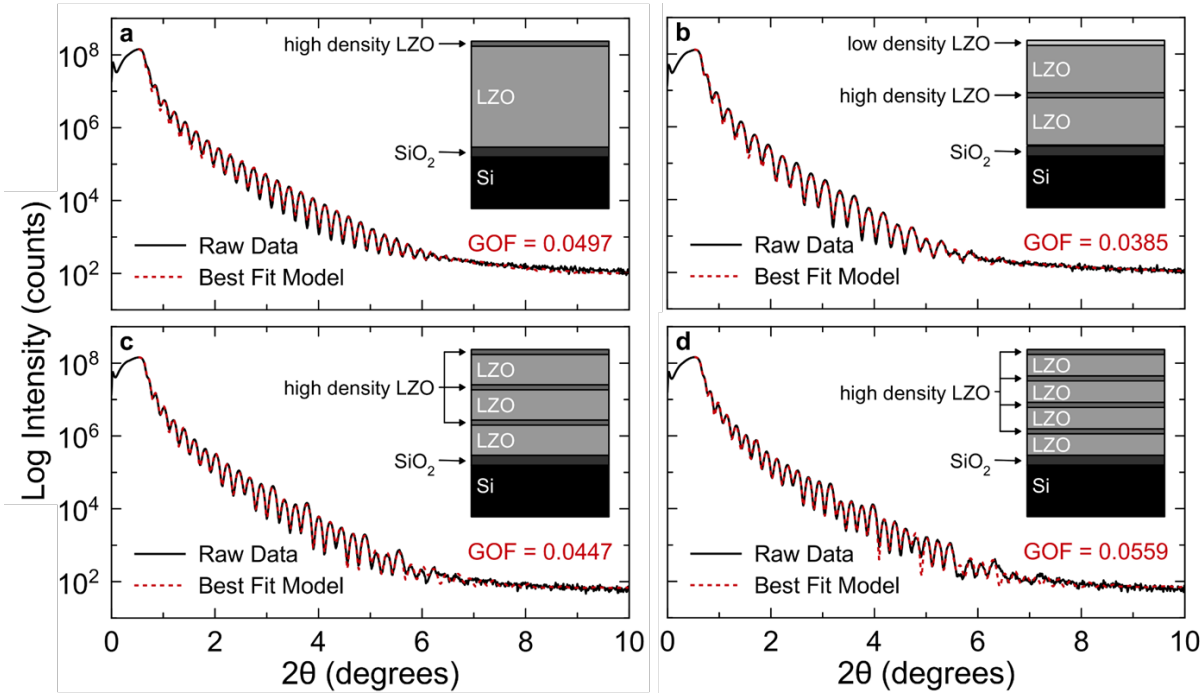

Figure S3. Multilayer models fit to XRR data collected from (a) one-, (b) two-, (c) three-, and (d) four-coat films deposited from 1.00, 0.50, 0.33, and 0.25 M precursor solutions, respectively. Starting models were informed by HAADF-STEM images in Figure 2.

Table S2: XRR multilayer best fit model parameters

	Multilayer Best Fit Parameters		
Layer(s)	***t* (nm)**	***D* (g cm^{-3})**	***R* (nm)**
1L Film			
LZO 1	1.71	5.79	0.3
LZO 2	36.2	5.36	0.1
2L Film			
LZO 1	0.9	5.02	0.3
LZO 2	13.1	5.85	0.1
LZO 3	1.1	5.71	0.3
LZO 4	16.1	5.89	0.2
3L Film			
LZO 1	1.8	5.89	0.4
LZO 2	12.6	5.71	0.1
LZO 3	1.2	6.02	0.2
LZO 4	13.1	5.78	0.3
LZO 5	1.3	6.04	0.2
LZO 6	9.2	5.86	0.1
4L Film			
LZO 1	1.8	6.03	0.4
LZO 2	9.9	5.63	0.7
LZO 3	1.3	6.00	0.1
LZO 4	9.8	5.62	0.8
LZO 5	1.2	6.00	0.1
LZO 6	10.0	5.69	0.8
LZO 7	1.3	6.04	0.1
LZO 8	6.6	5.91	0.3

Table S2. XRR multilayer best fit model parameters [thickness (*t*), density (*D*), roughness(*R*)] for XRR data and models presented in Figure S3.

Figure S4: Energy-dispersive X-ray spectroscopy (EDS) measurements

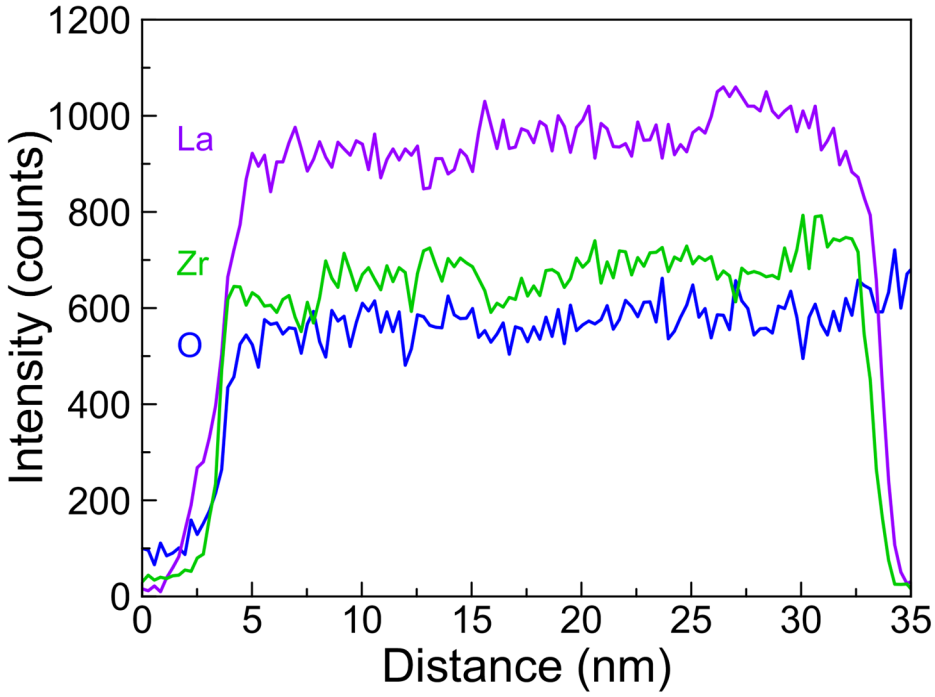

Figure S4. Cross-sectional STEM-EDS profiles from a three-layer LZO film deposited from a 0.33 M precursor solution. Intensity profiles plotted are the O Kα, La Lα, and Zr Lα signals vs. distance from the film surface (where a distance of zero is the film surface).

Table S3: Electron probe microanalysis (EPMA) measurements

Precursor Molarity	Layers	La at%	Zr at%	N at%	O at%	La/Zr	(La+Zr)/O	(La+Zr)/(O+N)
1.00	1	14.8(1)	14.6(1)	5.6(5)	65.1(3)	1.01(1)	0.45(1)	0.42(1)
0.50	2	15.3(2)	15.2(1)	3.8(6)	65.7(4)	1.01(2)	0.46(1)	0.44(1)
0.33	3	15.5(1)	15.1(1)	2.9(4)	66.5(3)	1.03(1)	0.46(1)	0.44(1)
0.25	4	15.9(1)	15.6(1)	2.4(6)	66.2(6)	1.02(1)	0.48(1)	0.46(1)

Table S3. Atomic ratios measured using EPMA with 95% confidence intervals from 5 EPMA measurements (uncertainty indicated in parentheses).

Figure S5: Medium energy ion scattering (MEIS) data and best fit model

He ions that scatter from larger masses are detected at higher energies. Therefore, the highest energy peak corresponds to ions backscattered from La in the film, while the lower energy peak corresponds to ions backscattered from Zr.

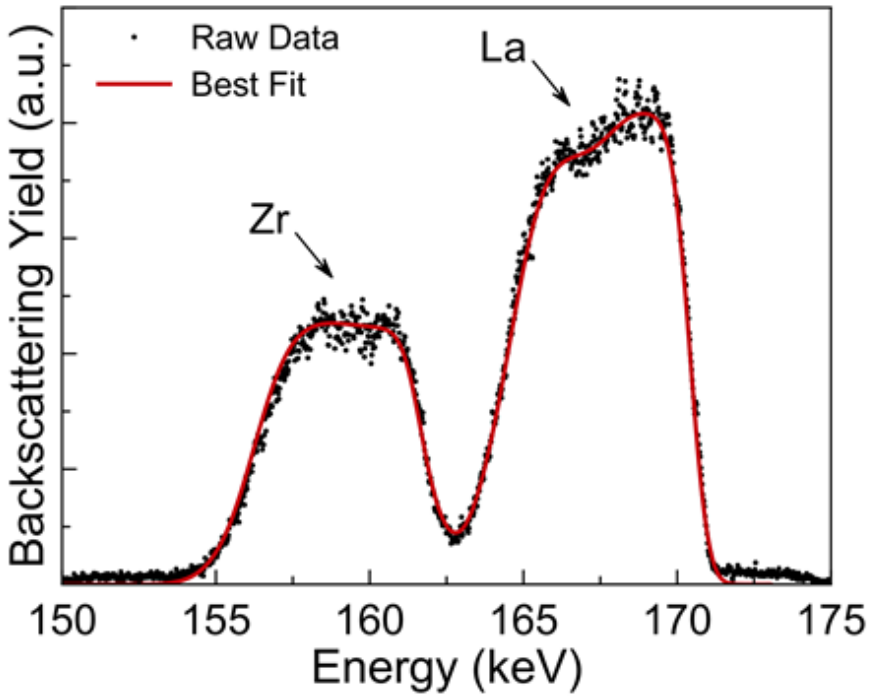

Figure S5: MEIS experimental data (black) collected from a thin two-layer (~8 nm) film overlaid with the best fit model (red) indicates a surface enrichment of La, whereas the amount of Zr throughout the film is essentially constant.

Table S4: X-ray photoelectron spectroscopy (XPS) measurements

Films were sputtered with 1 keV Ar^+ ions for a total of three minutes (~3-4 nm). The composition was determined by using XPS peak area analysis in the MultiPak Software.

	Air-Annealed LZO film	
Sputter (s)	**La 3d (%)**	**Zr 3d (%)**
0	57.5	42.5
5	62.6	37.4
30	62.1	37.9
60	59.4	40.6
180	57.2	42.8

Table S4. Relative La and Zr atomic percentages for a one-layer LZO film deposited from a 0.33 M precursor solution and annealed to 450 °C in an ambient environment.